EGTRIB Journal
JOURNAL OF
THE EGYPTIAN SOCIETY OF TRIBOLOGY
VOLUME 14, No. 4, October 2017, pp. 40 - 53 **ISSN 2090 - 5882**
(Received July 25. 2017, Accepted in final form September 18. 2017)

TRIBOLOGICAL PROPERTIES OF LOW DENSITY POLYETHYLENE AND POLYAMIDE 12 AS POLYMER MATRIX NANOCOMPOSITES

Hassan A. El-Sayed M. [1], EiD A. I.[2], El-Sheikh M.[1] and Ali W. Y.[3]

[1]Mechanical Dept., Faculty of Industrial Education, Beni-Suef University, Beni-Suef, Egypt.
[2]Composite Materials Lab., Advanced Materials Division, Central Metallurgical Research and Development Institute "CMRDI", Helwan, Cairo, Egypt.
[3]Production Engineering and Mechanical Design Dept., Faculty of Engineering, El-Minia University, El-Minia, Egypt.

ABSTRACT
Polymeric nanocomposites (PNCs) have solved many problems due to their extensive applications such as aerospace, automobiles, coatings, and packaging materials. In the present study, low density polyethylene (LDPE) and polyamide 12 (PA12), as a matrix materials reinforced with graphene nanoplatelets (GNPs), impregnated by paraffin oil (PO) were fabricated by a hot compression technique. Tribological properties of unfilled LDPE, PA12, and their nanocomposites have been investigated by pin-on-disc tester at a constant sliding distance of 212 m and 1.2 m/s sliding speed under 20 N applied normal load. Tribological properties proved that LDPE/GNPs and PA12/GNPs nanocomposites have lower coefficient of friction (COF), and wear rates compared with pure LDPE and PA12. By adding PO contents to the LDPE and its nanocomposites, COF and wear rates were gradually increased. Also, after PO addition to unfilled PA12/GNPs and PA12/GNPs nanocomposites, COF and wear rates gradually decreased. Worn surfaces were imaged using scanning electron microscope (SEM).

KEYWORDS
Low density polyethylene, polyamide 12, graphene nanoplatelets, paraffin oil, polymeric nanocomposites, tribological properties.

INTRODUCTION
Nanocomposite materials with nanofiller have emerged in the last few decades as a promising class of materials, which take the advantage of greatly higher specific surface area, higher loads, and controlled interfacial interactions, [1]. LDPE, polypropylene (PP), polystyrene (PS), and many other polymers can be used in packaging applications, [2 - 4]. PNCs materials have solved many problems due to their extensive applications such as aerospace, automobiles, coatings, packaging materials, and construction engineering. Many researches have focused on the use of natural materials in the polymer nanocomposites as fillers, [5, 6]. Filler materials play an effective role in improvement of composite properties. Selecting size and shape of filler, filler types and

loadings, optimum filler-matrix ratio, compatibility between matrix and filler interfacial bonds, and well filler distribution, lead to improvement the composite performance, [7]. The uniform distribution of nanofiller in the polymer matrix can improve electrical, thermal, mechanical, flame retardant, and gas barrier properties of the nanocomposite materials [5]. Nanofillers such as carbon nanofibers (CNFs), carbon nanotubes (CNTs), and exfoliated graphite (EG) are the most common fillers which used for preparing the polymer nanocomposites [8], [9]. Kuila et al., found that CNTs are very effective conductive fillers in thermal, electrical, and mechanical properties. However, CNTs have high production cost which limits their applications as nanofiller, [5, 10].

The most common nanofillers such as carbon nanofibers (CNFs), carbon nanotubes (CNTs), and exfoliated graphite (EG) can be used for preparing the (PNCs), [8, 9]. Carbon nanotubes (CNTs) are very effective conductive fillers in thermal, electrical, and mechanical properties. However, carbon nanotubes (CNTs) have high production cost which limits their applications as nanofiller, [5, 10]. Graphene discovery in 2004 has largely overcome this problem, [11]. Graphene is well known for its unique properties such as excellent mechanical properties (tensile strength ~ 130 GPa and elastic modulus ~ 0.5-1 TPa), high specific surface area, high aspect ratio and has exceptional thermal, mechanical, and electrical properties. These unique properties make graphene suitable for composite materials field and many technological applications, including sensors, energy storage, electronic circuits, and solar cells, [12 –15]. In addition, one important application of graphene is using it as a reinforcement material in polymer matrix nanocomposites, [16]. Recent studies which conducted on the use of graphene as nanofiller, showed that it may be the best among other traditional nanofiller because of its unique properties, [8].

The dispersion of graphene is an important factor to enhancement of polymer properties. There are three main blending techniques for the fabrication of polymer/graphene nanocomposites: melt mixing, solution blending, and in situ polymerization [12]. Among these three common techniques, melt mixing is the most environmentally and economically because it does not require any solvents and this process can be carried out using mechanical mixing equipment, [17, 19]. Thermoplastic engineering polymers have attracted attention in industrial applications, and enhancement in their mechanical and physical properties will widen this horizon [20]. Mechanical characteristics of (PNCs) based on thermoplastic matrix material can be enhanced using graphene as a reinforcement material [16, 21].

Improving the tribological properties of the polymeric composites can be achieved using nanofibers and nanoparticles, [7]. Wear characteristics of polymer matrix nanocomposites are dependent on the materials properties and the sliding conditions, such as lubricating conditions, environment, and counterface materials, [22]. Although many researches have been conducted on enhancing the tribological properties of polymer matrix nanocomposites by adding many fillers, there are few researches about reducing the wear of polymer composites by varying the sliding parameters, [23]. The tribological properties of short carbon fiber (SCF) /PA66 and SCF/epoxy polymer composites were reported, [24, 25] and found that the composite properties were

enhanced by adding 5 vol. % of TiO_2 as a reinforcement nanoparticles. Incorporation of multi-walled carbon nano- tubes (MWCNT) in PP as a polymer matrix was studied by Dike et al. and showed an improvement in polypropylene wear resistance and mechanical properties. MWCNTs with low filler concentrations showed a similar effect on wear resistance after adding to epoxy composites, in study done by Campo et al. [24]. Also, graphene oxide (GO) studies for reinforcement of polymer composites have proved that the tribological performance of polymeric matrices have been improved.

The polyamide 6 / glass fiber composites filled with single graphite, ultrahigh molecular weight polyethylene (UHMWPE), polytetrafluoroethylene (PTFE), and their complex solid lubricants were studied, [26], and showed an enhancement in the mechanical and tribological properties of these composites. The addition of solid lubricant such as polytetrafluoroethylene (PTFE), ultrahigh molecular weight polyethylene (UHMWPE) and graphite into (PNCs) has the advantage of self-lubricating behavior, thus it can help in prevention of instabilities of stick-slip motion, thus the COF and wear rate characteristics were improved, [26, 29]. LDPE, which is within the PE family, has attracted extensive attention in scientific studies due to the more flexible processing compared to high density PE, and good balance between strength and rigidity, [10, 14].

The aim of the present work is to introduce new self-lubricating polymeric nanomaterials for bearing applications and manufacture of fast and cheap polymeric dies. There have been some studies reported on improving the mechanical performance of LDPE/GNPs composites, [30, 32]. However, there have been no studies on the tribological performance of LDPE/GNPs composites. Therefore, this work interested on studying the effect of different filler loadings of GNPs and PO, as a liquid lubricant material, on the tribological properties of LDPE and PA12 nanocomposites.

EXPERIMENTAL

Materials

The matrix material, composed of powdered LDPE and PA12. LDPE was supplied from Saudi Arabia Basic Industries Corporation (SABIC), with an average particle size of 279.8 nm. PA12 was supplied from EOS company, North America, with an average particle size of 22.3 nm. The average particle size of LDPE and PA12 was identified by means of laser diffractometry using Zeta Sizer nano-series (nano ZS). GNPs, used as a reinforcement material, have 2 - 10 nm thickness, 20 - 40 m^2/g specific surface area, and average particle diameter of ~ 5 µm. GNPs were obtained from ACS MATERIALS Company, USA. Figure 1 shows scanning electron microscope image of GNPs as received from the company data sheet. A medical grade of PO was used in manufacturing of the composites at different weight fractions (wt. %) to study its effects on the mechanical and tribological properties of nanocomposites.

Nanocomposites Preparation

A hot compression technique at a compression pressure of 0.3 MPa was employed to produce the pure LDPE, PA12, and their nanocomposites. Specimens were prepared with the mass ratios (GNPs: LDPE or PA12) of 0, 0.25, 0.5, 0.75, and 1 wt. %. All of these nanocomposites were fabricated with 0, 2.5, 5, 7.5, and 10 wt. % of PO. The

nanocomposites were mixed and heated for 10 minutes at temperature of 150°C in a cylindrical pressing die. This pressing die was manufactured by M238 hot working steel, which has an internal diameter of 6.5 mm as shown in Fig. 2. After temperature had reached to 135 °C, for LDPE, and 200 °C, for PA12, nanocomposites were hot pressed by a hydraulic pressing system, as presented in Fig. 3. Then, the specimens were cooled gradually to room temperature. Finally, specimens dimensions of 6.5 mm in diameter and 45 mm in length were cut into suitable sizes for further tests.

Characterization Methods

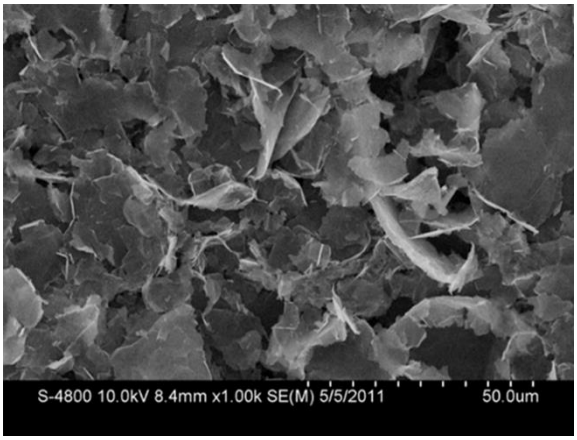

Fig. 1 SEM of as received GNPs.

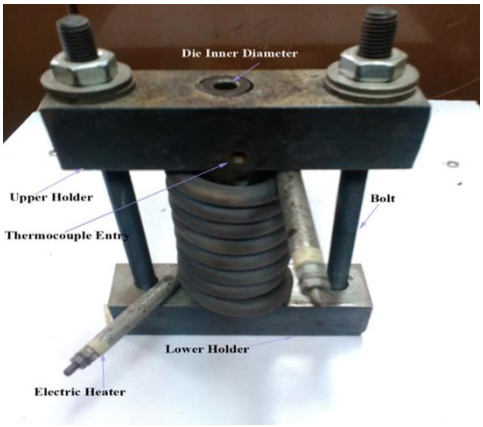

Fig. 2 Pressing die.

Fig. 3 Hydraulic pressing system.

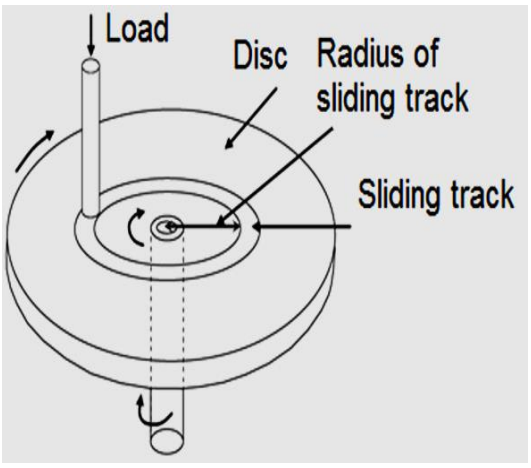

Fig. 4 Schematic diagram of pin-on-disc test rig.

Figure 4 shows a pin-on-disc test rig used for sliding wear experiments. Wear test was conducted on LDPE, PA12, and their composites by using carbon steel disc to act as a sliding counterface in accordance with ASTM standard G99, [33]. The specimens were cut into pin shapes with dimensions of 6.5 mm in diameter and 30 mm in length. The steel disc has dimensions of 185 mm diameter, 8 mm thickness, surface hardness of 58-62 HV, and surface roughness (Ra) of 1.11 µm. For PA12 and its nanocomposites,

aluminum oxide (alumina) abrasive paper of grit 1000 (Ra = ~ 4.6 µm) was glued onto a carbon steel disc surface to act as a sliding counterface.
Wear test was performed on a track diameter of 150 mm for specified sliding distance, sliding speed, and applied normal load. The test was carried out at 30 ± 3 °C by an applied normal load of 20 N and run for a constant sliding distance and sliding speed of 212 m and 1.2 m/s, respectively. Specimens were weighed before and after the wear test using a digital electronic balance, which has ± 0.1 mg accuracy. Difference between specimen weights represented the wear rate. The averaged values of at least three tests for each specimen were reported.

During the wear test, friction force was measured continuously throughout the wear test using a load cell of 40 kg. A load cell was connected to the calibrated data logger, which recorded the friction force each one millisecond, and their average values were introduced. COF was calculated by dividing the friction force by an applied normal force. The microstructure and worn surfaces of the composites were examined by SEM.

RESULTS AND DISCUSSION
The experimental results of COF of unfilled LDPE, PA12, and their nanocomposites were introduced in Fig. 5 and Fig. 6, respectively. According to variations of COF versus GNPs wt. % in absence of PO content as indicated in Fig. 5, GNPs reduced COF of unfilled LDPE by 0.51, 0.97, 1.49, and 3.18 % at 0.25, 0.5, 0.75, and 1 wt. % GNPs contents, respectively. Also, as indicated in Fig. 6, GNPs reduced COF of unfilled PA12 by 8.35, 10.6, 12.57, and 22.67 % at 0.25, 0.5, 0.75, and 1 wt. % GNPs contents, respectively. COF of the nanocomposites as shown in Fig. 5 and Fig. 6 showed slightly decreasing trend by addition of GNPs. It is known that GNPs have a very low COF, so that adding GNPs into LDPE and PA12 can obtain nanocomposites with a lower COF. On the other hand, GNPs can be readily dragged out from the polymeric matrix to form a third-body transfer film, which leads to reduce the direct contact between the polymeric matrix and abrasive asperities counterface.

By adding PO of 2.5, 5, 7.5, and 10 wt. % contents to unfilled LDPE and LDPE/GNPs nanocomposites, COF increased gradually with increasing PO content. When PO content increased up to 10 wt. %, COF of LDPE increased by 4.035, 3.76, 4.14, 4.54, and 6.27 % at 0, 0.25, 0.5, 0.75, and 1 wt. % GNPs, respectively, as shown in Fig. 5. This may be attributed to the weak interaction between PO and LDPE/GNPs composites, which caused the emergence of porosity as indicated in SEM examination, Fig. 9d. However, in all cases of PO contents, GNPs reduced the COF of LDPE/PO composites compared to unfilled LDPE and followed the same decreasing trend.

In the meantime, after addition of PO contents of 2.5, 5, 7.5, and 10 wt. % to unfilled PA12 and PA12/GNPs nanocomposites, COF showed significant enhancement by increasing PO content. When PO content increased up to 10 wt. %, COF of PA12 reduced by 49.47, 50.52, 51.02, 59.84, and 69.30 % at 0, 0.25, 0.5, 0.75, and 1 wt. % GNPs, respectively, as shown in Fig. 6. This may due to GNPs have a very low COF and they could be used as a solid lubricating material, where PO acted as a liquid lubricating

material, so that adding of GNPs and PO into PA12 led to obtain a new nanocomposite materials that has a lower COF with a self-lubricating characteristic.

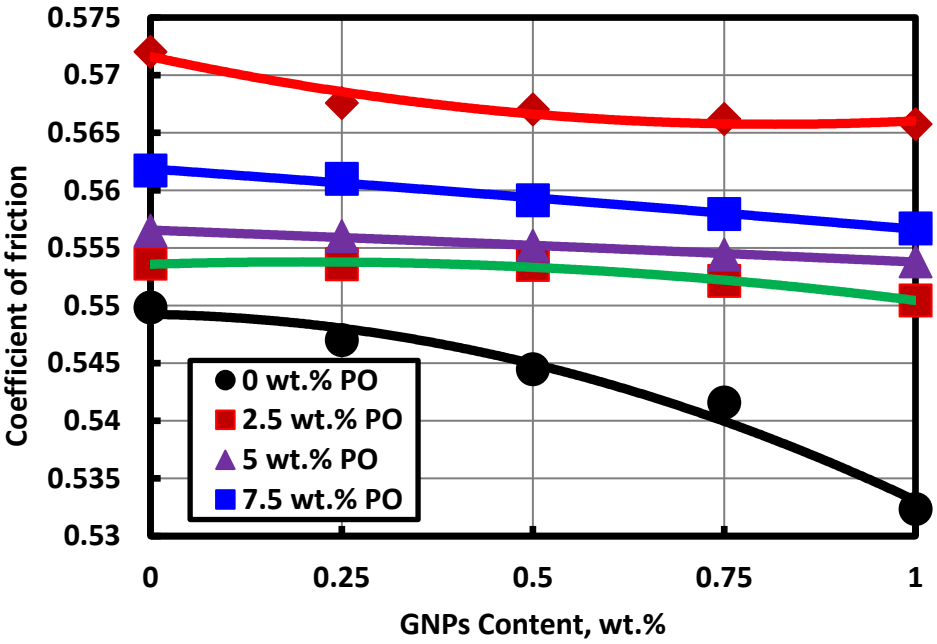

Fig. 5 COF of pure LDPE and its nanocomposites.

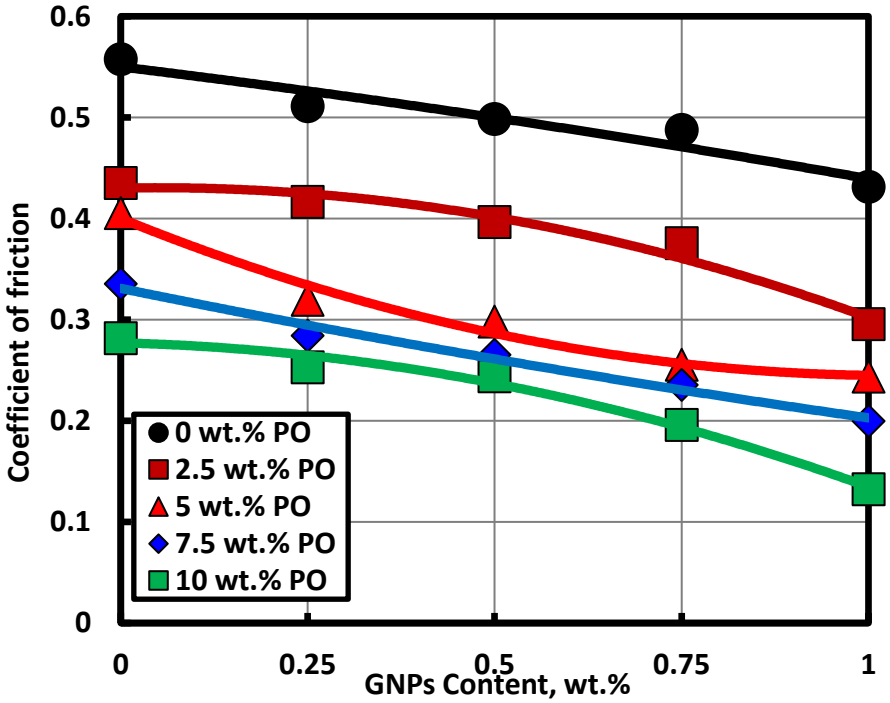

Fig. 6 COF of pure PA12 and its nanocomposites.

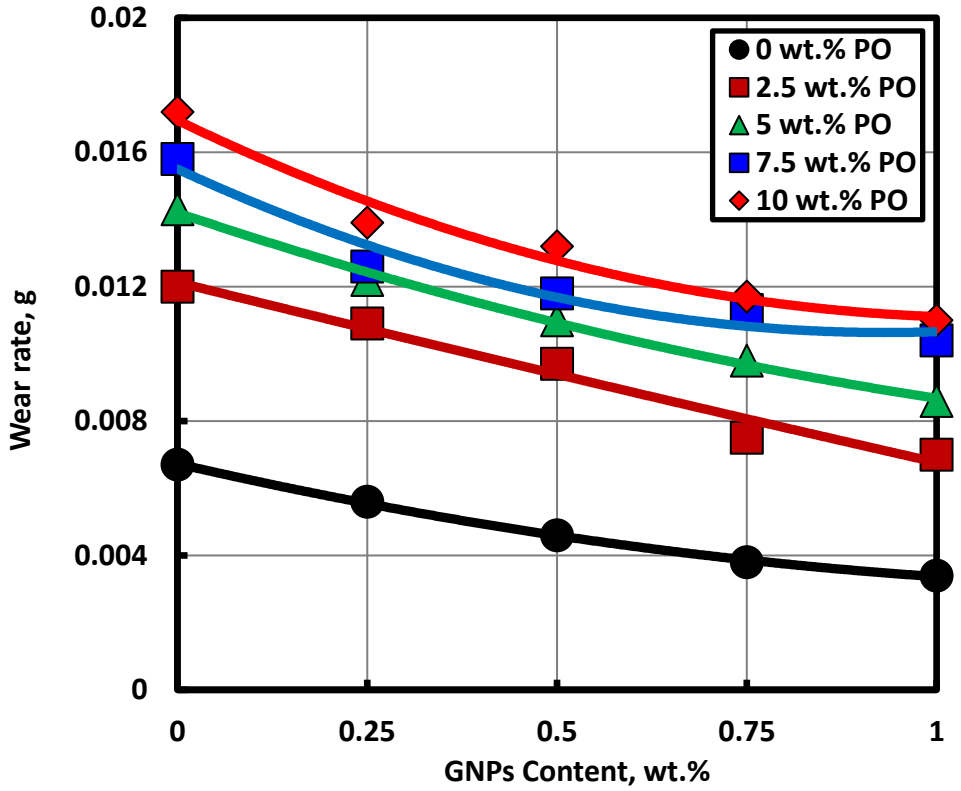

Fig. 7 Wear rate of pure LDPE and its nanocomposites.

Wear rate as a function of GNPs of unfilled LDPE, PA12, and their nanocomposites under dry sliding conditions were introduced in Fig. 7 and Fig. 8, respectively. As shown in Fig. 7, wear rate of LDPE was reduced by 16.42, 31.34, 43.28, and 49.25 % at GNPs contents of 0.25, 0.5, 0.75, and 1 wt. %, respectively. The wear rate was lower with 1.0 wt. % of GNPs. Generally, LDPE/GNPs nanocomposites exhibit decreased tendency of wear rate in dry sliding against the steel counterpart when the GNPs content is increased. According to variations of wear rate versus GNPs wt. % in absence of PO content as indicated in Fig. 8, GNPs reduced the wear rate of unfilled PA12 by 14.15, 21.23, 36.28, and 44.24 % at 0.25, 0.5, 0.75, and 1 wt. % GNPs, respectively. Because of high thermal conductivity and high strength of GNPs, the wear resistance has been improved due to transmission of frictional heat of nanocomposites and enhancement of the load carrying capacity [34]. Therefore, GNPs play an important role in improving the wear resistance and reducing of COF of LDPE and PA12.

After addition of PO to unfilled LDPE and LDPE/GNPs nanocomposites at contents of 2.5, 5, 7.5, and 10 wt. %, the wear rate of nanocomposites showed gradually increasing trend compared with LDPE/GNPs nanocomposites without PO. When PO content increased up to 10 wt. %, wear rate of LDPE increased by 79.1, 94.64, 110.86, 97.36, and 105.88 % at 0, 0.25, 0.5, 0.75, and 1 wt. %

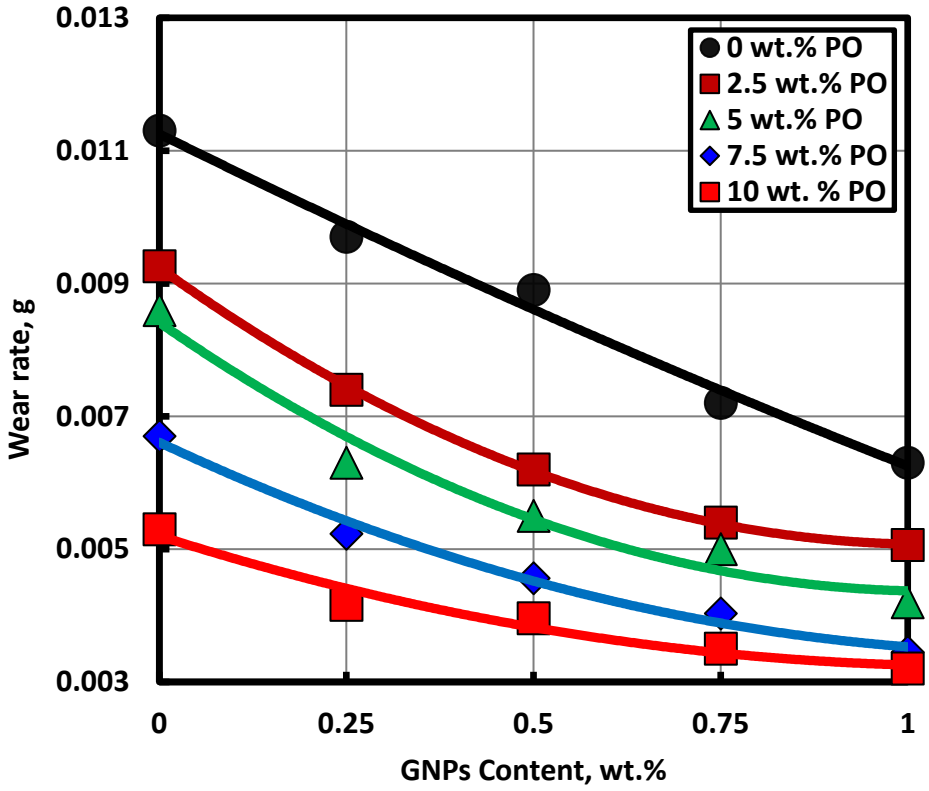

Fig. 8 Wear rate of pure PA12 and its nanocomposites.

GNPs, respectively, as shown in Fig. 7. This may be attributed to the weak interaction between PO and LDPE/GNPs composites that caused the emergence of porosity as indicated in SEM examination, Fig. 9d. However, in all cases of PO contents, GNPs reduced the COF of LDPE/PO composites compared to unfilled LDPE and followed the same decreasing trend

Wear rate of unfilled PA12 and PA12/GNPs nanocomposites at PO contents of 2.5, 5, 7.5, and 10 wt. % were presented in Fig. 8. It is clear that wear rate showed gradual decrease by increasing PO content. When PO content increased up to 10 wt. %, wear rate of PA12 decreased by 49.47, 50.52, 51.02, 59.84, and 69.3 % at 0, 0.25, 0.5, 0.75, and 1 wt. % GNPs, respectively as shown in Fig. 8. Generally, PA12/GNPs/PO nanocomposites exhibit decreased tendency of wear rate in dry sliding against abrasive alumina counterface when the GNPs and PO contents increased. Recent studies emphasized that this significant improvement of tribological performance of PNCs may be attributed to the transfer film formation, which protects the steel or abrasive counterpart and specimens then leads to reduce the ability of wear rate and COF, [35], [36 - 38]. Composites with more uniform transfer films had lower COF and wear rates, [38]. Hence, these transfer films were responsible for enhancement of the tribological performance of GNPs reinforced LDPE and PA12. It may be considered that, at the start of the wear test, the sliding surface of LDPE and its nanocomposites comes in

contact with the rough steel disc, and the sliding surface of PA12 and its nanocomposites comes in contact with the alumina abrasive counterface. The surface asperities of the steel disc and the abrasive counterface have been adhered by transfer film, which was removed from the specimen surface under the influence of load and sliding speed. With the formation of uniform and coherent transfer film, a new stage begins where the sliding occurs between LDPE/GNPs and PA12/GNPs nanocomposites, then the transfer film covering the steel disc and abrasive counterface surface. Consequently, low COF and wear rate have been obtained. In consideration of the low COF and wear rate, LDPE + 1 wt. % GNPs and PA12 + 1 wt. % GNPs + 10 wt. % PO nanocomposites could be used as promising materials for the tribological applications in dry sliding against steel and abrasive materials such as alumina.

The comparison on the worn surface of both the unfilled LDPE, LDPE/1wt. % GNPs, and LDPE/1wt. % GNPs/10 wt. % PO were characterized using SEM images as shown in Fig. 9 a, c, and d. While the worn surface of the unfilled PA12, PA12/1wt. % GNPs, and PA12/1wt. % GNPs/10 wt. % PO were introduced in Fig. 10 a, c, and d. As indicated in Fig. 9a, the worn surface of the unfilled LDPE contains more ploughed marks, which illustrated that the wear mechanism was distinguished with adhesive and ploughing wear. Because of the increased temperature at contacted surfaces, severe adhesive wear occurred mainly due to the softening of the unfilled LDPE. Moreover, the ploughed marks and fractures on the worn surfaces of the composites were caused by the micro-cutting and micro-ploughing action from the abrasive asperities counterface.

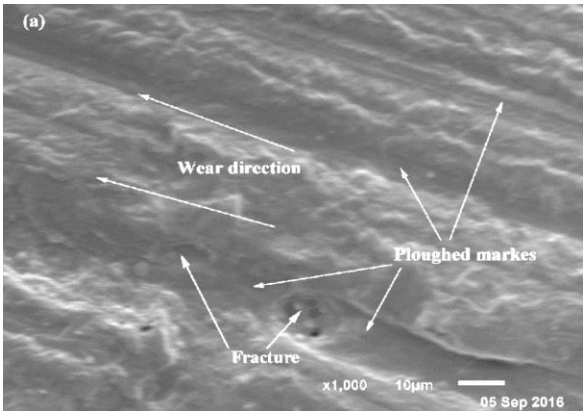

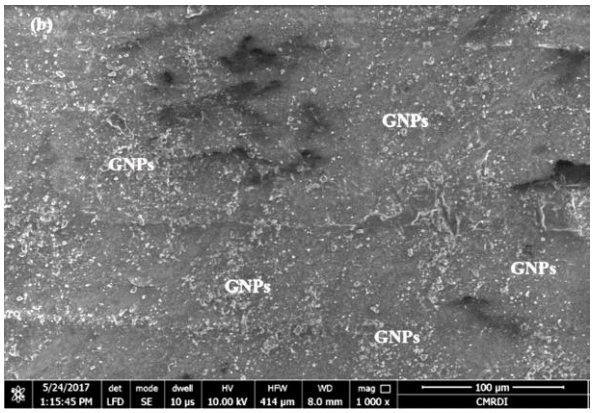

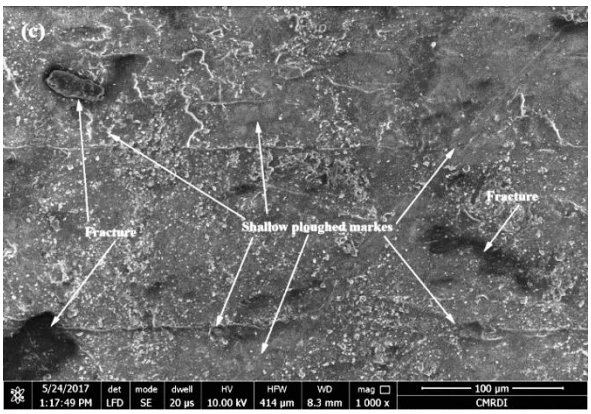

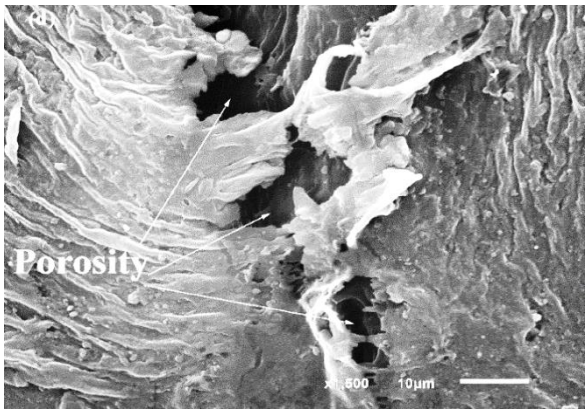

Fig. 9 SEM micrographs of the worn surface of: (a) pure LDPE after wear, (b) LDPE+1wt.% GNPs before wear, (c) LDPE+1wt.% GNPs after wear, and (d) LDPE+1wt.% GNPs+10% PO after wear.

Also, the worn surface of the unfilled PA12 contains more ploughed marks, which illustrated that the wear mechanism was distinguished with abrasive and ploughing wear as shown in Fig. 10a. The ploughed marks and fractures on the worn surfaces were caused by the micro-cutting and micro-ploughing action from the abrasive alumina counterface.

Distribution of 1wt. % GNPs in LDPE and PA12 matrix, as shown in Fig. 9b and Fig.10b, resulted in a high surface mechanical strength of LDPE/1wt. % GNPs and PA12/1wt. % GNPs nanocomposites. The high surface mechanical strength of these nanocomposites helped in preventing deeper wear grooves during sliding action. Besides surface properties, the transfer films formed during sliding also played a significant role in controlling the wear behavior of the materials [7].

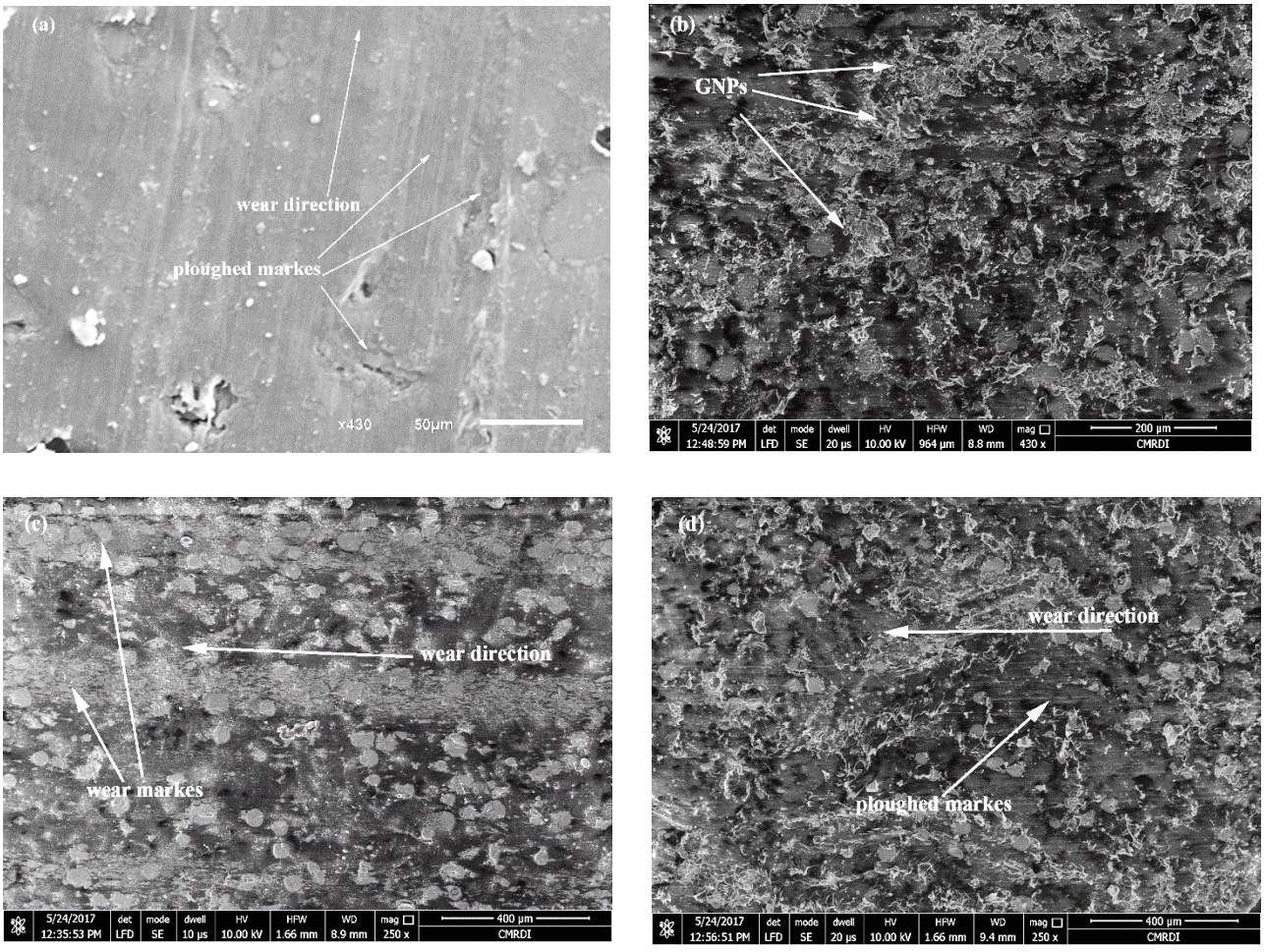

Fig. 10 SEM micrographs of the worn surface of: (a) pure PA12 after wear, (b) PA12+1wt.% GNPs before wear, (c) PA12+1wt.% GNPs after wear, and (d) PA12+1wt.% GNPs+10% PO after wear.

During the sliding process, these GNPs were easily released from the LDPE/GNPs and PA12/GNPs nanocomposites, then transferred to LDPE and PA12 nanocomposites contact zone and the counterface. Thus, the GNPs could work as a solid lubricant material between the two contacted surfaces and prevent the direct contacting between them, thereby reduce the COF and increase the wear resistance. This resulted in less wear or ploughed marks and shallower grooves of LDPE/1wt. % GNPs and PA12/1wt. % GNPs worn surfaces, as shown in Fig. 9c and 10c. Hence, the LDPE/1wt. % GNPs and PA12/1wt. % GNPs nanocomposites showed much better friction and wear resistance compared with unfilled LDPE and PA12. As for the worn surface of LDPE/1wt. % GNPs filled with 10 wt.% PO as shown in Fig. 9d, the porosity was shown clearly on the surface which led to weak interaction between PO and LDPE/GNPs nanocomposites. Thereby, increasing of wear rate and COF with increasing PO content may be attributed to the porosity formation, which led to weak interaction between PO and LDPE/GNPs nanocomposites.

The worn surfaces of PA12/1wt. % GNPs after adding of 10 wt. % PO seemed to be smoother than those at unfilled PA12/1wt. % GNPs and PA12/1wt. % GNPs composites. This may be attributed to the increase in the shear resistance of PA12 provided by GNPs and PO contents as shown in Fig. 10d. During the sliding process, GNPs with PO would be ploughed and transferred from the matrix to the abrasive counterface surface. Then, the wear debris of GNPs and PO accumulated on the counterface surface and formed a dynamic transfer film. When the transfer film was formed, it could effectively reduce the direct contact area of abrasive counterface and PA12 surface, and cause the sliding process between them. This behavior is very much consistent with COF and wear rate obtained from PA12/GNPs/PO compared to the unfilled PA12. According to the analysis of the tribological behaviors, nanocomposites composed of PA12/1 wt. % GNPs/10 wt. % PO could be used as a self-lubricating material under dry sliding condition.

CONCLUSIONS

In the present study, LDPE and PA12 matrix nanocomposites reinforced with GNPs and PO were fabricated and the tribological properties of these nanocomposites were investigated. COF and wear rate of unfilled LDPE and PA12 were decreased with increasing of GNPs wt. %. This may be attributed to the transfer film formation that protects the steel and abrasive counterface disc, and GNPs that have very low COF and high surface mechanical strength. Therefore, the GNPs play an important role in improving the wear resistance and reducing COF of LDPE and PA12. After addition of PO to LDPE/GNPs nanocomposites at loadings of 2.5, 5, 7.5, and 10 wt. %, the COF and wear rate of nanocomposites showed gradually increasing trend compared to LDPE/GNPs nanocomposites without PO contents. This may be attributed to the weak interaction between PO and LDPE/GNPs nanocomposites that caused porosity formation was gradually increased. After addition of PO to PA12/GNPs nanocomposites at contents of 2.5, 5, 7.5, and 10 wt. %, the COF and wear rate of nanocomposites showed decreased with increasing of GNPs and PO wt. %. This may be due to the transfer film formation, which protects the specimens' surfaces and covers the surface of the abrasive counterface. Therefore, GNPs, as a solid lubricant, and PO, as a liquid

lubricant, play an important role in improving the wear resistance and reducing COF of PA12. The tribological results that discussed in this study could potentially aid in rational design and the use of self-lubricating nanocomposites.

ACKNOWLEDGEMENT

This research was supported by production technology department in faculty of industrial education, Beni-Suef University, Egypt, and composite materials Lab., Central Metallurgical Research and Development Institute "CMRDI", Helwan, Cairo, Egypt.

REFERENCES

1. Hu K., Kulkarni D. D., Choi I., and Tsukruk V. V., "Graphene-polymer nanocomposites for structural and functional applications," Prog. Polym. Sci., Vol. 39, No. 11, pp. 1934 – 1972, (2014).

2. Luyt A. S. and Geethamma V. G., "Effect of oxidized paraffin wax on the thermal and mechanical properties of linear low-density polyethylene-layered silicate nanocomposites," Polym. Test., vol. 26, no. 4, pp. 461–470, (2007).

3. Goudarzi M. D., Salavati-Niasari M., and Ahmadi A., "Sonochemical Synthesis of Spherical Silica Nanoparticles and Polymeric Nanocomposites," J. Clust. Sci., vol. 27, no. 1, pp. 25–38, (2016).

4. Cui Y., Kundalwal S. I., Kumar S., "Gas barrier performance of graphene/polymer nanocomposites," Carbon N. Y., vol. 98, pp. 313–333, (2016).

5. Kuila T., Bose S., Mishra A. K., Khanra P., Kim N. H., and Lee J. H., "Effect of functionalized graphene on the physical properties of linear low density polyethylene nanocomposites," Polym. Test., vol. 31, no. 1, pp. 31–38, (2012).

6. Verma D., Gope P. C., Shandilya A., and Gupta A., "Mechanical-Thermal-Electrical and Morphological Properties of Graphene Reinforced Polymer Composites: A Review," Trans. Indian Inst. Met., vol. 67, pp. 803–816, (2014).

7. Chang B. P., Akil H. M., Affendy M. G., Khan A., and Nasir R. B. M., "Comparative study of wear performance of particulate and fiber-reinforced nano-ZnO/Ultra-high molecular weight polyethylene hybrid composites using response surface methodology," Mater. Des., vol. 63, no. August, pp. 805–819, (2014).

8. Kuilla T., Bhadra S., Yao D., Kim N. H., Bose S., Lee J. H., "Recent advances in graphene based polymer composites," Prog. Polym. Sci., vol. 35, no. 11, pp. 1350–1375, (2010).

9. Goodridge R. D. et al., "Processing of a Polyamide-12/carbon nanofibre composite by laser sintering," Polym. Test., vol. 30, no. 1, pp. 94–100, (2011).

10. Kuila T. et al., "Preparation of functionalized graphene/linear low density polyethylene composites by a solution mixing method," Carbon N. Y., vol. 49, no. 3, pp. 1033–1037, (2011).

11. Dhand V., Rhee K. Y., Kim H. J., and Jung D. H., "A Comprehensive Review of Graphene Nanocomposites : Research Status and Trends," Journal of Biomaterials, vol. 2013, (2017).

12. Kim H. et al., "Graphene/polyethylene nanocomposites: Effect of polyethylene functionalization and blending methods," Polymer (Guildf)., vol. 52, no. 8, pp. 1837–1846, (2011).

13. Das T. K. and Prusty S., "Graphene-Based Polymer Composites and Their Applications," Polym. Plast. Technol. Eng., vol. 52, no. 4, pp. 319–331 , (2013).
14. Lahiri D., Hec F., Thiesse M., Durygin A., Zhang C., and Agarwal A., "Nanotribological behavior of graphene nanoplatelet reinforced ultra high molecular weight polyethylene composites," Tribol. Int., vol. 70, pp. 165–169, (2014).
15. Vermisoglou E. C. et al., "Graphene-based materials via benzidine-assisted exfoliation and reduction of graphite oxide and their electrochemical properties," Appl. Surf. Sci., vol. 392, pp. 244–255, (2017).
16. Zhang H. B. et al., "Electrically conductive polyethylene terephthalate/graphene nanocomposites prepared by melt compounding," Polymer (Guildf)., vol. 51, no. 5, pp. 1191–1196, (2010).
17. Lee J. H., Kim S. K., and Kim N. H., "Effects of the addition of multi-walled carbon nanotubes on the positive temperature coefficient characteristics of carbon-black-filled high-density polyethylene nanocomposites," Scr. Mater., vol. 55, no. 12, pp. 1119–1122, (2006).
18. Sengupta R., Bhattacharya M., Bandyopadhyay S., and Bhowmick A. K., "A review on the mechanical and electrical properties of graphite and modified graphite reinforced polymer composites," Prog. Polym. Sci., vol. 36, no. 5, pp. 638–670, (2011).
19. Phiri J., Gane P., and Maloney T. C., "General overview of graphene: Production, properties and application in polymer composites," Mater. Sci. Eng. B, vol. 215, pp. 9–28, (2017).
20. Chatterjee S., Nüesch F. A., and Chu B. T. T., "Comparing carbon nanotubes and graphene nanoplatelets as reinforcements in polyamide 12 composites.," Nanotechnology, vol. 22, no. 27, p. 275714, (2011).
21. Rafiq R., Cai D., Jin J., and Song M., "Increasing the toughness of nylon 12 by the incorporation of functionalized graphene," Carbon N. Y., vol. 48, no. 15, pp. 4309–4314, (2010).
22. Chang L., Zhang Z., Breidt C., and Friedrich K., "Tribological properties of epoxy nanocomposites I. Enhancement of the wear resistance by nano-TiO_2 particles," Wear, vol. 258, no. 1–4 SPEC. ISS., pp. 141–148, (2005).
23. Chang L. and Friedrich K., "Enhancement effect of nanoparticles on the sliding wear of short fiber-reinforced polymer composites: A critical discussion of wear mechanisms," Tribol. Int., vol. 43, no. 12, pp. 2355–2364, (2010).
24. Campo M., Jiménez-Suárez A., and Ureña A., "Effect of type, percentage and dispersion method of multi-walled carbon nanotubes on tribological properties of epoxy composites," Wear, vol. 324–325, pp. 100–108, (2015).
25. Min C., Nie P., Song H. J., Zhang Z., and Zhao K., "Study of tribological properties of polyimide/graphene oxide nanocomposite films under seawater-lubricated condition," Tribol. Int., vol. 80, pp. 131–140, (2014).
26. Li D., Xie Y., Li W., You Y., and Deng X., "Tribological and mechanical behaviors of polyamide 6/glass fiber composite filled with various solid lubricants," Sci. World J., vol. 2013, (2013).
27. Bijwe J., Sen S., and Ghosh A., "Influence of PTFE content in PEEK-PTFE blends on mechanical properties and tribo-performance in various wear modes," Wear, vol. 258, no. 10, pp. 1536–1542, (2005).

28. Zhang G., Rasheva Z., and Schlarb A. K., "Friction and wear variations of short carbon fiber (SCF)/PTFE/graphite (10 vol.%) filled PEEK: Effects of fiber orientation and nominal contact pressure," Wear, vol. 268, no. 7–8, pp. 893–899, (2010).
29. Hashmi S. A. R., Neogi S., Pandey A., and Chand N., "Sliding wear of PP/UHMWPE blends: Effect of blend composition," Wear, vol. 247, no. 1, pp. 9–14, (2001).
30. Lei H. et al., "Graphene enhanced low-density polyethylene by pretreatment and melt compounding," RSC Adv., vol. 6, no. 103, pp. 101492–101500, (2016).
31. Fim F. D. C. Basso N. R. S., Graebin A. P., Azambuja D. S., and Galland G. B., "Thermal, electrical, and mechanical properties of polyethylene-graphene nanocomposites obtained by in situ polymerization," J. Appl. Polym. Sci., vol. 128, no. 5, pp. 2630–2637,(2013).
32. Gaska K., Xu X., Gubanski S., Kádár R., "Electrical, mechanical, and thermal properties of LDPE graphene nanoplatelets composites produced by means of melt extrusion process," Polymers (Basel)., vol. 9, no. 1, pp. 30–40, (2017).
33. Sahin Y., "Analysis of abrasive wear behavior of PTFE composite using Taguchi's technique," Cogent Eng., vol. l, pp. 1–15, (2015).
34. Pan B. et al., "Tribological and mechanical investigation of MC nylon reinforced by modified graphene oxide," Wear, vol. 294–295, pp. 395–401, (2012).
35. Chang B. P., Akil H. M,, Nasir R. B., and Khan A., "Optimization on wear performance of UHMWPE composites using response surface methodology," Tribol. Int., vol. 88, pp. 252–262, (2015).
36. Guo C., Zhang Z. Z., Liu W., Su F., and Zhang H., "Influence of Solid Lubricant Reinforcement on Wear Behavior of Kevlar Fabric Composites," Appl. Polym. Sci., vol. 110, pp. 1771–1777, (2008).
37. Li Y., Wang Q., Wang T., and Pan G., "Preparation and tribological properties of graphene oxide/nitrile rubber nanocomposites," J. Mater. Sci., vol. 47, no. 2, pp. 730–738, (2012).
38. Liu H., Li Y., Wang T., and Wang Q., "In situ synthesis and thermal, tribological properties of thermosetting polyimide/graphene oxide nanocomposites," J. Mater. Sci., vol. 47, no. 4, pp. 1867–1874, (2012).